

## Study of the effect of imperfect tips on nanoindentation by FEM

Feng-Yuan Chen<sup>1,\*</sup> and Rwei-Ching Chang<sup>2</sup>

<sup>1</sup>*Department of Mechanical Engineering, Lee-Ming Institute of Technology, Taiwan*

<sup>2</sup>*Department of Mechanical and Computer-Aided Engineering, St. John's University, Taiwan*

(Manuscript Received May 31, 2007; Revised August 30, 2007; Accepted September 30, 2007)

---

### Abstract

In this paper, the imperfect tip effect of the Ti film on Si substrate on nanoindentation with Berkovich probe tip was investigated with the finite element method (FEM). In the literature, we found the effects of tip deformation and tip radius on nanoindentation were investigated frequently, but the imperfect centerline of tip has never been studied. In this work, at first, the Ti film on Si substrate was conducted with a high-resolution nanomechanical test. The Young's modulus of Ti films can be obtained by using the Oliver and Pharr method while the nanoindentation depth is smaller than 20% of the film thickness for avoiding the substrate effect. Second, the FEM was employed to determine the yield stress of thin films because it cannot be found from nanoindentation. Finally, the load-depth of nanoindentation was compared between the experimental data and numerical results. The results show while choosing the suitable yield stress of films, the load-depth curves of numerical simulation were very close to the experimental curves with the imperfect effect being ignored. Moreover, it is concluded while the imperfect angles of tip were considered that the larger imperfect angles  $|\theta_z|$  or  $\theta_x$ , the smaller displacement on nanoindentation.

*Keywords:* Nanoindentation; FEM; thin film; Imperfect tips

---

### 1. Introduction

In recent year, the mechanical surface properties of many materials can be improved by depositing an appropriate thin film and the techniques have been developed and used for tribological applications. Because the deformation of coated surfaces produced by tribological interactions can result in substantial damage, it is very important to quantify the resistance of the material to such damage. For this reason the evaluation of the mechanical properties of thin films is of fundamental importance. The elasticity modulus and hardness can be determined by using nanoindentation, but yield stress and other material properties cannot be obtained. For determining the

yield stress and other material properties, the numerical simulation is a powerful tool in the nanoindentation.

Due to the obvious mathematical complexity to analyze the nanoindentation process, the finite element is required and is an important role in recent technology developments and has been proved as a powerful tool in the nanoindentation simulation. Lichinchi et al. [1] used FEM to simulate nanoindentation of TiN film on HSS by using a commercial finite element code ABAQUS, and both axisymmetric and three-dimensional models were employed. They compared the experimental load-depth curves of titanium nitride thin film on high speed steel substrates with numerical results. Successively, they studied the effect of substrate on the hardness measurement and concluded that both models are similar and provide good fit. Ma et al. [2]

---

\*Corresponding author. Tel.: +886 2 29097811 (2262)

Fax.: +886 2 22966301

E-mail address: fychen@ms11.hinet.net

employed the finite element method for elastoplastic large strain to simulate the indentation test for Al film on Si substrate, and a hybrid method was presented to determine the mechanical properties of the films by combining calculation with nanoindentation test. Bai et al. [3] used the finite element method to simulate the nanoindentation process. The effect of internal stress on hardness and elastic modulus was investigated by nanoindentation simulation with the FEM. The experiment results and calculation results were further explained by contact mechanics analysis.

Pelletier et al. [4] have investigated the influence of bilinear elastic-plastic behaviour model for numerical simulation of nanoindentation testing of various bulk metals. They employed an axisymmetric rigid cone and equal volume to the Berkovich pyramid indenter to simulate the test. The indenter and the specimen were treated as a revolution body in order to have three-dimensional situation. The numerical simulation results of loads versus displacement compare reasonably well to experimental results of nanoindentation tests of pure metals such Fe, Ni, Ti and A316L and TAFE alloys. However, they concluded that different pairs of yield strength and plastic modulus can produce a good fit to the experimental results of load versus displacement. Their explanation for this non-uniqueness of solution would be the bad definition of the indenter geometry and the adopted material behavior. Bouzakis et al. [5-7] developed a procedure to extract constitutive laws based on an evaluation of nanoindentation results through a developed continuous simulation of the indenter penetration into a coated specimen. Their algorithm considered nanoindentation results as input data to the described finite element model and extracts stress strain coating curves. For all their papers, the FEM simulation of nanoindentation, due to accuracy reasons, is based on an axisymmetric FEM model.

Meanwhile, Jeong and Lee [8] studied the tip deformation and the error-in-hardness on nanoindentation by FEM. The tip deformation was analyzed in terms of the variance of normalized tip radius, which has the peak value at a certain indentation depth and does not depend on the tip radius. The equation for the calibrated hardness, which can be used to determine the correct hardness excluding the tip deformation effect, has been derived from the parametric fitting function. Kim et al. [9] have improved the indentation size effect model to

include the effect of indenter tip bluntness based on the geometrically driven dislocation theory. Warren [10] used experimental and FEA to study the effects of surface integrity and tip geometry.

In the literature, we found the effects of tip deformation and tip radius on nanoindentation were investigated frequently, but the imperfect centerline of tip has never been studied. In this paper, the finite element method for elasto-plastic large strain was used to simulate the test for Ti films nanoindentation Si substrate. The imperfect tip effects are employed in the FEM to reproduce the nanoindentation load-depth curves. The results compared with both calculation solution and experimental data.

## 2. Nanoindentation

The Ti film on Si substrate was studied with a high-resolution nanomechanical test instrument which is a nanoindenter (Triboscope, Hysitron) assembled on an atomic force microscope (Autoprobe, CP-Research), and a three side pyramidal Berkovich probe tip is used in the test. Five indentations were made in each sample at the same maximum loads. Nanoindentation is performed under a precisely continuous measurement of the load and the depth during the test. Fig. 1 shows a schematic draw of an indentation load via depth curve.

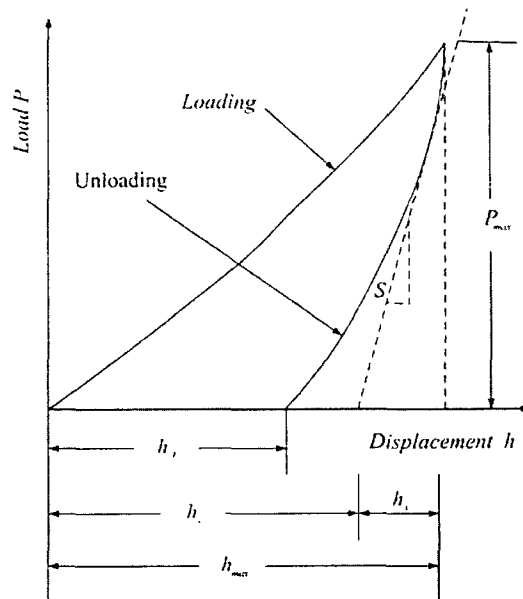


Fig. 1. Schematic representation for load-depth data for a nanoindentation experiment.

In the Oliver and Pharr [11] method, the hardness  $H$  and the reduced modulus  $E_r$  are derived from

$$H = \frac{P_{\max}}{A} \tag{1}$$

and

$$\left(\frac{dP}{dh}\right)_{\text{unload}} = S = 2\beta E_r \sqrt{\frac{A}{\pi}} \tag{2}$$

where  $P_{\max}$  is the maximum indentation load,  $A$  is the projected contact area,  $S$  is the unloading stiffness measured at maximum depth of penetration  $h$ ,  $\beta$  is a constant that depends on the geometry of the indenter for Berkovich indenter  $\beta=1.034$ . The reduced modulus is used in the analysis to take into account that elastic deformation occurs in both the indenter and the specimen and it is given by

$$\frac{1}{E_r} = \frac{1-\nu^2}{E} + \frac{1-\nu_i^2}{E_i} \tag{3}$$

where  $E$ ,  $E_i$  and  $\nu$ ,  $\nu_i$  are the elastic modulus and Poisson's ratio of the indenter and the specimen material, respectively. For evaluating the elastic modulus  $E_r$ , the slope  $\left(\frac{dP}{dh}\right)_{\text{unload}}$  and the contact area  $A$  should be determined precisely. A least mean square fit to 90% of the unloading curve is made according to the hypothesis that the unloading data will be expressed by a power law

$$P = P_{\max} \left(\frac{h-h_f}{h_{\max}-h_f}\right)^m \tag{4}$$

For an indenter with a known geometry, the projected contact area is a function of the contact depth. The area function for a perfect Berkovich indenter is given

by

$$A = f(h_c) = 24.56h_c^2 \tag{5}$$

Indenters used in practical nanoindentation testing are not ideally sharp. Therefore, tip geometry calibration or area function calibration is needed. A series of indentations is made on fused quartz at depths of interest. A plot of  $A$  versus  $h_c$  can be curve fit according to the following functional form

$$A = f(h_c) = 24.56h_c^2 + C_1h_c^1 + C_2h_c^{1/2} + C_3h_c^{1/4} + \dots + C_8h_c^{1/128} \tag{6}$$

where  $C_1$  through  $C_8$  are constants. The lead term describes a perfect Berkovich indenter.

### 3. Numerical simulation

The FEM has been widely used to simulate the nanoindentation process. In this study, a commercial finite element code ANSYS was used to determine the stress-strain curve of the Ti film on Si substrate with the nanoindentation and SOLID95, CONTA174 and TARGE170 elements were adopted. Fig. 2 shows the elements mesh and the contact region of both tip and thin film were finely meshed for good simulation accuracy. The Berkovich diamond tip is defined as perfectly elastic material. Young's modulus and Poisson's ratio are taken as 1140 GPa and 0.07, respectively [2]. The silicon substrate is defined as perfectly elastic material. Young's modulus and Poisson's ratio are taken as 127 GPa and 0.278, respectively [2]. The Ti film was assumed as elastic-perfectly plastic materials and Young's modulus were obtained by using the Oliver and Pharr method. Using FEM was found the yield stress because it cannot be obtained on nanoindentation. While the elastic-perfectly plastic material was employed at FEM, the

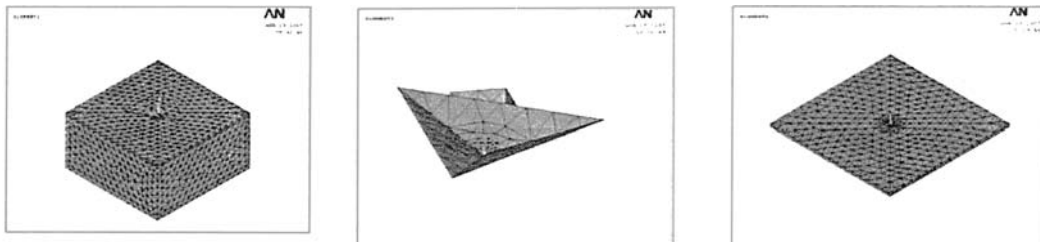


Fig. 2. The elements mesh.

yield stress must be changed for reproducing the experimental load-depth curve.

**4. Result and discussion**

The film and coating technologies have been developed for tribological applications. Because the hardness, yield stress and elasticity modulus are the basic parameters for mechanical design. It is very important to conduct the hardness, yield stress and elasticity modulus. Nanoindentation test is one of very important methods to evaluate the material properties of thin film. In the nanoindentation, the geometry of contact area between the indenter and the specimen during the indentation is of crucial importance in determining the resulting material properties. Therefore, in our work the imperfect centerline of tip was considered in nanoindentation (see Fig. 3), where  $\theta_x$ ,  $\theta_y$  and  $\theta_z$  are the imperfect angles due to misalignment of the centerline of tip. When the coordinate system is set at  $\theta_y = 0$  and there are two imperfect angles  $\theta_x$  and  $\theta_z$  will be studied.

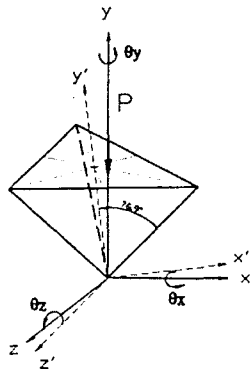


Fig. 3. The imperfect centerline of tip.

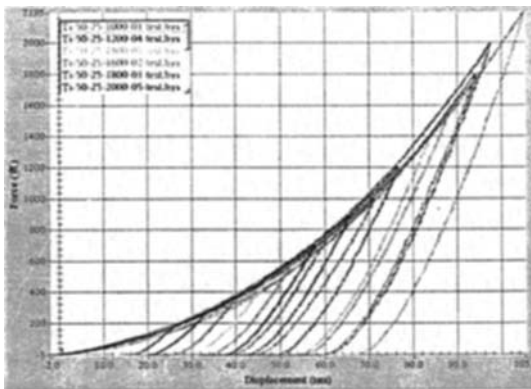


Fig. 4. The load-depth curves due to nanoindentation test.

At first, the Ti film on Si substrate were studied with a high-resolution nanomechanical test instrument which is a nanoindenter (Triboscope, Hysitron) assembled on an atomic force microscope (Autoprobe, CP-Research), and a three side pyramidal Berkovich probe tip is used in the test. Five indentations were made in each sample at the same maximum loads. Therefore, the nanoindentation testing is successfully and load-depth curve is performed in Fig. 4. There are a lot of experiments at maximum load from 150  $\mu N$  to 2200  $\mu N$ . But only the maximum load 150  $\mu N$  was considered in this paper, the thickness of Ti film was deposited to 200 nm, and the thickness of Si substrate was about 35  $\mu m$ , because the penetration depth is chosen not to exceed 20 % of the film thickness in order to avoid substrate effects [1].

Second, as reported by Oliver and Pharr [11], the elasticity modulus and hardness can be determined by their method in nanoindentation but yield stress and other material properties cannot be obtained. The elastic modulus E of the thin film introduced in the analysis is determined from Eqs. (1)-(6) as E=150 GPa, and the value of the Poisson's ratio found in the literature  $\nu = 0.25$  [2]. For determining the yield stress and other material properties, the finite element method is used to simulate the elastic and plastic deformation behavior in nanoindentation. In this research, the elasto-plastic large strain was used to simulate the nanoindentation test for Ti films on Si substrate and a hybrid method is present for producing the experimental load-depth curves, and the value of yield stress can be obtained by FEM and nanoindentation. The material properties are assumed as elastic-perfectly plastic (see Fig. 5) in which  $S_y$  is the yield stress.

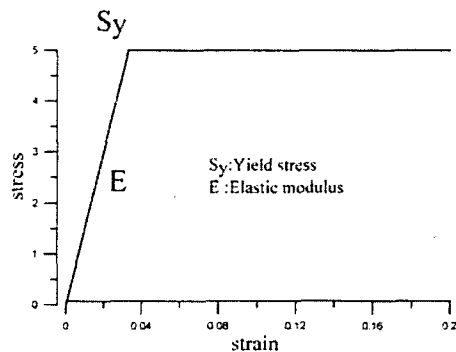


Fig. 5. The stress-strain curve of the elastic-perfectly plastic material.

Fig. 6 presents the load-depth curves in different yield stresses  $S_y$  (4, 5 and 6 GPa), where the linear elastic modulus is  $E = 150$  GPa and force is  $P_{max} = 150$   $\mu$ N. The solid line is the experimental data redrawn from Fig. 4. Comparison of the curves of numerical simulation with experimental curves shows that the loading and unloading curve of simulation by FEM shifts to the right as  $S_y \leq 5$  GPa. The smaller yield stress  $S_y$ , the more the curve shifts right. When  $S_y = 6$  GPa the loading curve of simulation by FEM is very close to the experimental curve as  $P > 50$   $\mu$ N. But the unloading curve of simulation by FEM shifts to the left and exists the large deviation. This may be due to differences in the actual and assumed yield stress or due to the use of a constitutive model of materials like elastic perfectly-plastic one without work-hardening rate or due to the rounding of the tip as a result of wear.

Finally, the different imperfect angles are considered and the coordinate system is set at  $\theta_y = 0$  and there are two imperfect angles  $\theta_x$  and  $\theta_z$  will

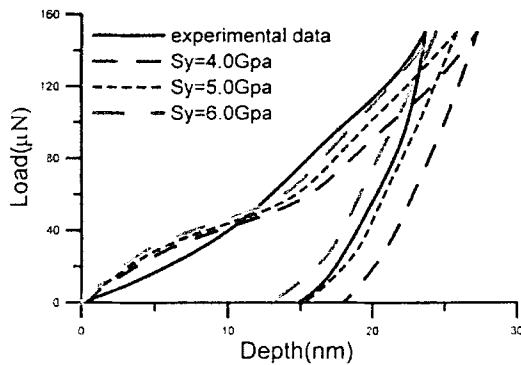


Fig. 6. The load-depth curves by nanotndentation and FEM in different yield stress  $S_y$ .

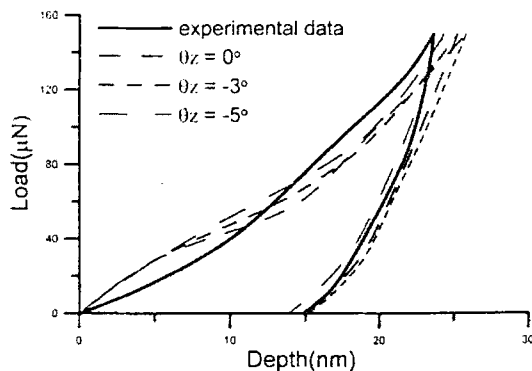


Fig. 7. The load-depth curves by nanotndentation and FEM in different imperfect angle and yield stress  $S_y = 5$  Gpa,  $\theta_x = 0^\circ$ .

be studied. Fig. 7 shows the load-depth curves in different imperfect angle  $\theta_x = 0^\circ$  and  $\theta_z = 0^\circ, -3^\circ$  and  $-5^\circ$ , at the yield stress  $S_y = 5$  GPa, where the linear elastic modulus is  $E = 150$  GPa, and force is  $P = 150$   $\mu$ N. It shows the loading and unloading curves of simulation by FEM shifts to the left while the imperfect angle  $\theta_z < 0^\circ$ . The larger the imperfect angle  $|\theta_z|$ , the more the curve shifts.

Fig. 8 shows the load-depth curves as different imperfect angles  $\theta_x = 0^\circ$  and  $\theta_z = 0^\circ, 3^\circ$  and  $5^\circ$ , at the yield stress  $S_y = 5$  GPa, where the linear elastic modulus is  $E = 150$  GPa, and force is  $P = 150$   $\mu$ N. It shows the loading and unloading curve of simulation by FEM shifts to the left while the imperfect angle  $\theta_z > 0^\circ$ . The larger the imperfect angle  $\theta_z$ , the more the curve shifts. When  $\theta_z = 5^\circ$  the loading curve of simulation by FEM shifts to the left and very close to the experimental curve. But the unloading curve of simulation by FEM shifts to the left and exists the large deviation. Due to Fig. 7 and Fig. 8, either  $\theta_z > 0^\circ$  or  $\theta_z < 0^\circ$  when the imperfect angles of tip were considered, the larger imperfect angles  $|\theta_z|$ , the smaller displacement on nanoindentation.

Fig. 9 shows the load-depth curves at different imperfect angles  $\theta_z = 0^\circ$  and  $\theta_x = 0^\circ, 3^\circ$  and  $5^\circ$ , at the yield stress  $S_y = 5$  GPa, where the linear elastic modulus is  $E = 150$  GPa, and force is  $P = 150$   $\mu$ N. It shows the loading and unloading curve of simulation by FEM shifts to the left while the imperfect angle  $\theta_x > 0^\circ$ . The larger the imperfect

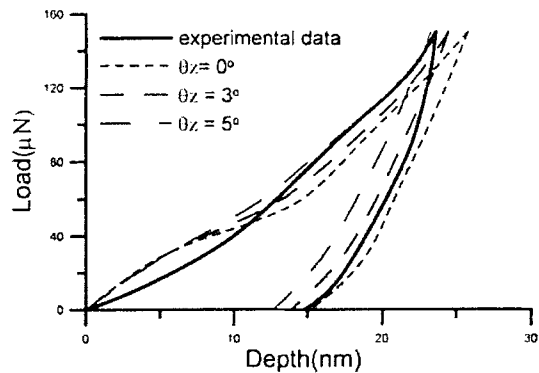


Fig. 8. The load-depth curves by nanotndentation and FEM in different imperfect angle and yield stress  $S_y = 5$  Gpa,  $\theta_x = 0^\circ$ .

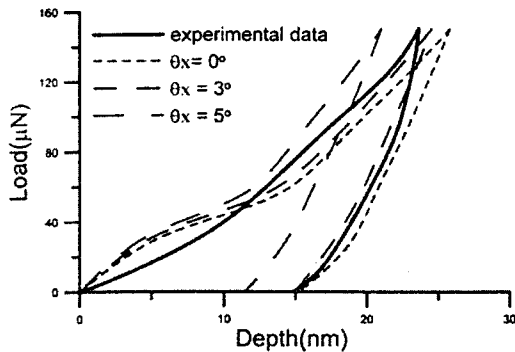


Fig. 9. The load-depth curves by nanoindentation and FEM in different imperfect angle and yield stress  $S_y=5\text{Gpa}$ ,  $\theta_z = 0^\circ$ .

angle  $\theta_x$ , the more the curve shifts. Therefore, while the imperfect angles  $\theta_x$  were considered, the larger imperfect angles  $\theta_x$ , the smaller displacement on nanoindentation.

According to the above discussion, using the FEM to reproduce the load-depth curves of nanoindentation was employed by different material properties. While the elastic-perfectly plastic material was used at numerical simulation and the yield stress  $S_y$  is 5Gpa, the load-depth curves of numerical simulation agree well with the experimental data. When the imperfect angles of tip were considered that the larger imperfect angles  $|\theta_z|$  or  $\theta_x$ , the smaller displacement on nanoindentation.

## 5. Conclusions

FEM simulation with the commercial software ANSYS provided important observations of the plastic behaviors and load-depth curves of nanoindentation test. Therefore, the nanoindentation test is simulated by FEM while the different imperfect angles are considered. The numerical results are compared with the experimental data, and the following conclusions are obtained.

Comparison between the experimental data and numerical results demonstrated that finite element approach is capable of reproducing the loading-unloading behavior of a nanoindentation test.

While the elastic-perfectly plastic material was used at numerical simulation and the yield stress  $S_y$  is 5Gpa, the load-depth curves of numerical simulation agree well with the experimental data.

When the imperfect angles of tip were considered that the larger imperfect angles  $|\theta_z|$  or  $\theta_x$  the smaller displacement on nanoindentation.

## 6. References

- [1] M. Lichinchi, C. Lenardi, J. Haupt and R. Vitali, Simulation of Berkovich nanoindentation experiments on thin films using finite element method, *Thin Solid Films*. 312 (1998) 240-248.
- [2] D. Ma, K. Xu and J. He, Numerical simulation for determining the mechanical properties of thin metal films using depth-sensing indentation technique, *Thin Solid Films*. 323 (1998) 183-187.
- [3] M. Bai, K. Kato, N. Umehara and Y. Miyake, Nanoindentation and FEM study of the effect of internal stress on micro/nano mechanical property of thin CNx films, *Thin Solid Films*. 377-378 (2000) 138-147.
- [4] H. Pelletier, J. Krier, A. Cornet and P. Mille, Limits of using bilinear stress-strain curve for finite element modeling of nanoindentation response on bulk materials, *Thin Solid Films*. 379 (2000) 147-155.
- [5] K. D. Bouzakis, N. Michailidis and G. Erkens, Thin hard coatings stress-strain curve determination through a FEM supported evaluation of nanoindentation test results, *Surface and Coatings Technology*. 142-144 (2001) 102-109.
- [6] K. D. Bouzakis and N. Michailidis, Coating elastic-plastic properties determined by mean of nanoindentation and FEM-supported evaluation algorithm, *Thin Solid Films*. 469-470 (2004) 227-232.
- [7] K. D. Bouzakis, N. Michailidis and G. Skordaris, Hardness determined by mean of a FEM-supported simulation of nanoindentation and applications in thin hard coating, *Surface and Coatings Technology*. 200 (2005) 867-871.
- [8] S. M. Jeong and H. L. Lee, Finite element analysis of the tip deformation effect on nanoindentation hardness, *Thin Solid Films*. 492 (2005) 173-179.
- [9] J. Y. Kim, B. W. Lee, D. T. Read and D. Kwon, Influence of tip bluntness on the size-dependent nanoindentation hardness, *Scripta Materialia*. 52 (2005) 353-358.
- [10] A. W. Warren and Y. B. Guo, Machined surface properties determined by nanoindentation: experimental and FEA studies on the effects of surface integrity and tip geometry, *Surface and Coatings Technology*. 201 (2006) 423-433.
- [11] W. C. Oliver and G.M. Pharr, An improved technique for determining hardness and elastic-modulus using load and displacement sensing indentation experiments, *J. Mater. Res.* 7 (1992) 1564-83.